IJFANS INTERNATIONAL JOURNAL OF FOOD AND NUTRITIONAL SCIENCES
ISSN PRINT 2319 1775 Online 2320 7876
Research Paper , Journal Volume 11, Iss 09, 2022

ELECTRICAL CHARACTERIZATION OF GLASS FIBER REINFORCED POLYMER (GFRP) COMPOSITES FOR FUTURE META SURFACE ANTENNA APPLICATIONS

[1]Babu Morigalla,[2]Dr.Venkata Subba Reddy E,[3]Mallikarjuna Memerla
[13]Assistant Professor,[2]Professor
Department Of Mechanical Engineering
Tadipatri Engineering College,Tadipatri,AP

ABSTRACT:
Inthispaper,the GlassFiberReinforcedPolymer(GFRP)compositesamplesareexploredinordertoevaluate their feasibility and adaptability for use in future metasurface antenna application. Multi-layer GFRP composite samples are fabricated with a proportionate ratio of resins and fiber usingVacuumAssistedResinTransferMolding(VARTM)technique.Ntypetowaveguide(WR-187)adapterspeciallydesignedforelectricalcharacterizationoftheseGFRPcompositesamplesisused. Thru-Reflect-Line (TRL) calibration technique is used for the test setup, and scattering parameters oftheseGFRPsamplesismeasuredbyusingthemanufacturedadapteralongwiththesampleholderonatwoport VectorNetworkAnalyzer(VNA).Relativepermittivityanddielectriclosstangentof GFRPcomposite samples are computed using Nicholson-Ross-Weir (NRW) and New Non-Iterativeconversionmethods.Thecomparativeanalysesofbothmethodsshowedaverygoodagreement betweenthem.TheGFRPsamplewiththelowestrelativepermittivityisshortlistedforitspossibleapplicationin futuremetasurfaceantenna
.

INRODUCTION :
Composite materials have gained popularity over the years, and are being frequently used in differentengineering applications, because of superior advantage over commercially available engineering materials [1].Compositesreinforcedwithfibersofeithersynt heticornaturalmaterialsasdemandforlightweight materialaregrowinginthemarket.Fiberreinforced polymercompositesnotonlyofferhighstrengthto weightratiobutalsoprovide good electrical properties, high fracture toughness, durability, excellent corrosion and thermalresistance. Additionally, synthetic fiber in raw form is quite cheaper compared to other commercially availablematerialsinproductforminthemarket [2].Glassfiberisoneofthemostcommonlyusedsyn theticfiberemployedinwidevarietyofapplications ,including but not limited to electronics, mechanical, construction, automotive, aerospace, biomedical andmarine [3–6]. Glass fibers under different class of families (S-glass, E-glass and D-glass etc) are used incombinationwithfillersandpolymermatricestofor mcompositeGlassFiberReinforcedPolymer(GFRP).GFRPareusedin differentelectronicapplications, such asterminals, connectors,industrialsandhouseholdplugs,switche s,andPrintedCircuitBoard(PCB)etc.Ithas apotentialofusinginthefieldofRF/Microwave. Recently,inthefieldofRF/Microwave,Metamaterial andMetasurfacestructuresaregainingpopularitydue toelectromagneticperformanceenhancement.Meta surfaceistypicallymanufacturedusingasmallsetofsc atterersinaregulararraythroughouttheregioninorder toobtaindesirableelectromagneticbehavior.Metasu rfacehaswidevarietyofpotentialapplicationsinthefi eldofelectromagnetics[7],includinguseofMetasurf acebasedantenna [8].Useof2DMetasurfaceinthefieldofantennaenhan cesantennasperformance rangingfromapertureefficiencyimprovement[9],fre quencyre-configuration [10],switchablepolarization [11],highgainandwidebandwidth [12–14].Presently, metasurface antenna usesCommercialoff-the-Shelf

ISSN PRINT 2319 1775 Online 2320 7876
Research Paper Journal Volume 11, Iss 09, 2022

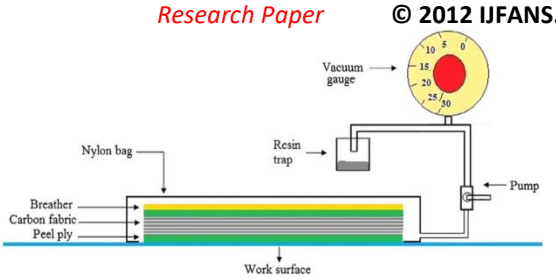

(COTS) based substrates [9–15]. These COTS based substrates are very expensive and can be replaced withGFRP based composite which are not only low cost but also offer good electrical and mechanical properties.

Atfirst,itisimportanttocharacterizeGFRPbasedcompositepolymersfortheirdielectricandmaterial properties.This is critical for the design of Metasurface and antenna structures on them [16]. An important feature of suchcomposite polymers is their ability to modulate their dielectric properties by varying the size, shape andconductivity of the filled constituent used in the polymeric matrix. Thus, the rationale of using GFRP basedpolymersinthedesignofreconfigurableantennas.

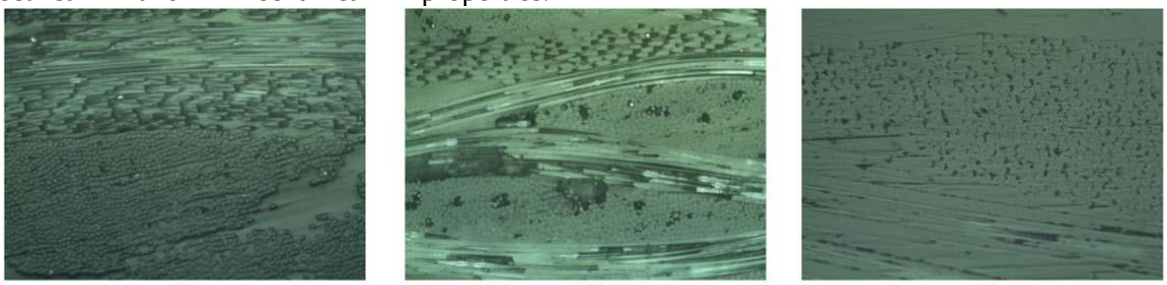

(a) (b) (c)

Table 1. Material composition of composite samples manufactured using VRATM technique.

Sample ID	Sample Image	Material Composition
X		**Reinforcement:** Chopped E-glass fibermat, Density 450 g m^{-2} sample thickness 2.32 mm. **Matrix:** Thermoset epoxy resin (Bisphenol-A) with hardener (Cycloaliphatic amine), Ratio of epoxy to hardener was kept 10:3.5 by weight. **Number of Layers:** 05 **Make (Matrix):** (Huntsman, Germany)
Y		**Reinforcement:** E-Glass fiber peel ply, Linear Density 200 g m^{-2}; Plain weave, sample thickness 2.62 mm. **Matrix:** Araldite GY 6010 epoxy resin with medium viscosity and high shelf life. **Number of Layers:** 15 **Make (Matrix):** (Huntsman, Germany)
Z		**Reinforcement:** Chopped E-glass fiber mat, Density 450 g m^{-2}, sample thickness 3.20 mm. **Matrix:** Araldite GY 6010 epoxy resin with medium viscosity and high shelf life. **Number of Layers:** 25 **Make (Matrix):** (Huntsman, Germany)

ISSN PRINT 2319 1775 Online 2320 7876
 Journal Volume 11, Iss 09, 2022

In this paper, manufacturing of GFRP composite samples is done using VARTM technique [21] and
scattering parameters of the manufactured samples are measured on a Vector Network Analyzer using TRL
method [23]. NRW [24, 25] and new non-iterative conversion methods are used to compute the relative permittivity and dielectric loss tangent of each sample. One of the composite samples with the lowest relative
permittivity will be then used for potential usage in metasurface antenna applications. In the past, antenna designers have used COTS based substrates[9–15] as metasurface. In this paper, we propose a novel idea of using an indigenously developed GFRP composite as a metasurface in antenna applications.

2. MANUFACTURING OF GFRP COMPOSITE SAMPLES

Manufacturing of composite samples is done using chopped E-glass fibermat and E-glass fiber peel ply cloth.
Fiber reinforced composite samples are fabricated through VARTM technique. For this purpose, a metallic plate is cleaned with acetone, and wax is applied on it for easy release of the mold after sample curing. Multiple numbers of sheets of glass fabric are stacked upon each other on a metallic plate. Then a polyester peel ply is placed over the layers of glass fabric, and a breather cloth is placed underneath it. An airtight nylon bag is positioned over the entire setup and a vacuum pump is attached to generate a constant vacuum pressure of 0.8 bars for 1 h. Schematic illustration of the VARTM technique is shown in figure 1.
Leaks are checked properly before switching on the vacuum pump. Plastic pipes are used as medium for resin infusion and vacuum generation, while tacky tape is used for mold sealing and vacuum retention purpose.
After the process, pump is switched off, while keeping the composites under vacuum for sample curing. Several samples with different configurations(change of number of layers and glass fiber) are manufactured. After the detailed scrutiny of all samples, 03 samples(Sample-X, Sample-Y and Sample-Z) of different thickness are short listed and discussed in this paper. All 03 samples are cured by heating the sample 30 min at 80 °C, 30 min at 120 °C and 2 h at 160 °C. Different number of layers is used in each sample resulting in different sample thicknesses. In this manner, the influence of varying number of layers on electromagnetic behavior will be studied in present article. The cured composite samples are removed and cut to desired dimensions for
characterization. All samples are fabricated via similar method; however reinforcement and matrix materials are changed according to table 1.
Composite samples(X, Y, Z) are subjected to optical microscopy for microstructural investigation. For optical microscopy, samples are prepared by following the standard grinding and polishing technique to obtain flat smooth surface. Images are captured at ×200 magnification using optical microscope (Optkia, Italy) and representative micrographs are shown in figure 2. As can be seen in the optical micrographs, fibermat and fiber ply are placed in three different orientations(0°, 45°, 90°). Images also illustrate proper manufacturing of samples with no voids and delamination defects. These samples can now be further used for their electrical characterization.

3. ELECTRICAL CHARACTERIZATION OF GFRP COMPOSITE SAMPLES

Manufactured GFRP composite samples are electrically characterized for determination of scattering parameters(S11, S12, S21, S22) using a 2 port Vector Network Analyzer(VNA). Characterization has been performed in C-band, i.e. 5.4 to 5.9 GHz. C-band measurement test components include TRL Reflect standard, TRL Thru standard/sample holder, N type to waveguide adapter(WR-187) and N-type to SMA adapter, as shown in figure 3(b). Sample holder and N-type to Waveguide

ISSN PRINT 2319 1775 Online 2320 7876
 Journal Volume 11, Iss 09, 2022

adapter(WR-187) are specifically designed and fabricated to carry out the testing activity. VNA is calibrated before carrying out the measurements, in order to avoid amplitude and phase errors.

Several calibration techniques can be used ranging from TRM (Thru-Reflect-Match), TRL (Thru-Reflect-Line), LRL (Line-Reflect-Line), LRM (Line-Reflect-Match) or SOLT (Short-Open-Line-Transmission). In the current scenario, 2-port Thru-Reflect-Line (TRL) calibration is performed to calibrate the setup in order to avoid any amplitude and phase errors in the measurement data of the samples[27]. After calibration is performed, Sample-Y is fitted in a sample holder as shown in figure 3(a). The sample holder is then sandwiched between the 02 C-band frequency waveguide adapter flanges, as shown in figure 3(c), to measure the scattering parameters.

Measured scattering parameters are saved in touchstone format in order to perform offline post processing, i.e. computing the relative permittivity (εr) and dielectric loss tangent (tanδ) of the composite samples. Same measurement procedure is repeated for Sample-X and Sample-Z for acquiring the S-parameters.

Scattering parameters of each sample are analyzed to evaluate the manufacturing quality as well as the effect of increasing number of layers from Sample-X to Sample-Z. Figure 4 exhibits plots of scattering parameters for all three samples.

Figures 4(a) and (b) depict measured Reflection Coefficients(S11) at Port 1 and (S22) at Port 2. Both S11 and S22 plots shows similarity for each sample with minimum reflection of energy for Sample-X due to less number of layers(05) and maximum reflection of energy for Sample-Z due to high number of layers(25). Similarity of S11 and S22 plots also indicates that both ends of the surface finish of each sample are smooth with no such perturbations or waviness. Similarly, figures 4(c) and (d) depicts Forward Transmission Coefficient(S12) and Reverse Transmission Coefficient(S21), which shows understandably maximum energy is passing though Sample-X having less number of layers(05), and minimum energy is passing through Sample-Z due to maximum number of layers(25). S12 and S21 plots also show uniform energy power level throughout the frequency band indicating no wavelength of the signal within the band is affected. Smooth scattering parameter plots with no glitches in the complete frequency band indicate proper manufacturing of both composite samples and test adapters. Now we can proceed for the calculation of relative permittivity (εr) and dielectric loss tangent(tanδ).

ISSN PRINT 2319 1775 Online 2320 7876
 Journal Volume 11, Iss 09, 2022

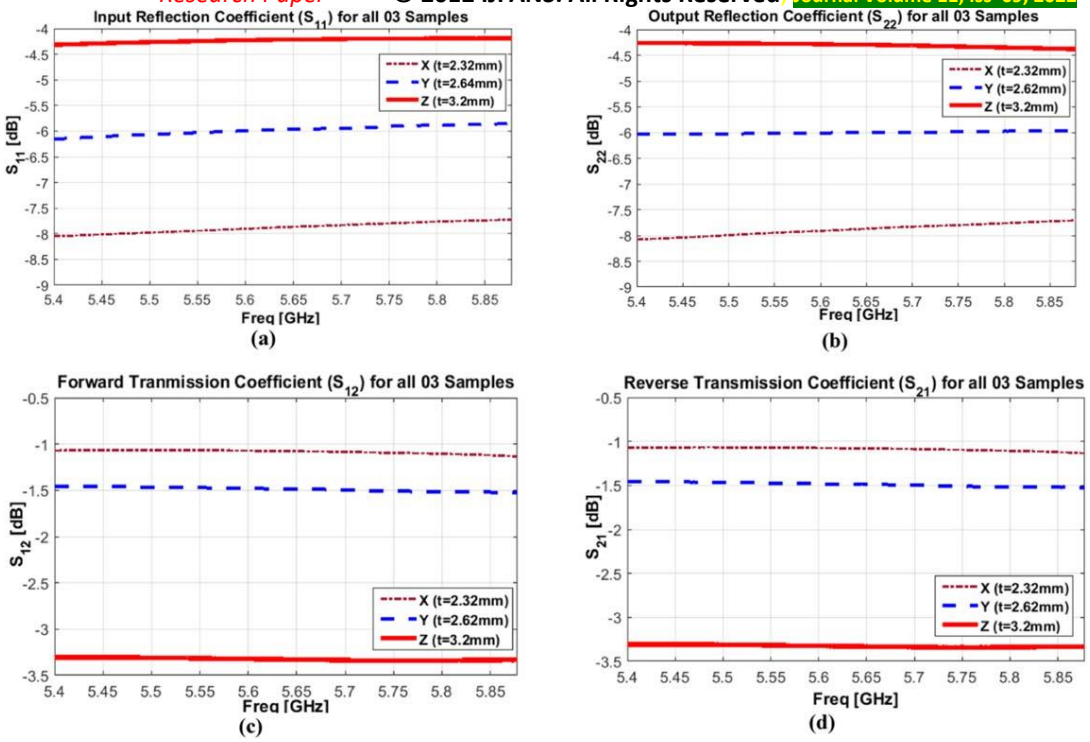

perturbations or waviness. Similarly, figures 4(c) and (d) depicts Forward Transmission Coefficient(S12) and Reverse Transmission Coefficient(S21), which shows understandably maximum energy is passing though Sample-X having less number of layers(05), and minimum energy is passing through Sample-Z due to maximum number of layers(25). S12 and S21 plots also show uniform energy power level throughout the frequency band indicating no wavelength of the signal within the band is affected. Smooth scattering parameter plots with no Selection of convergence methods are based on few factors which includes type of measurement method adopted for calculating the scattering parameters, type of material used, speed and accuracy of convergence methods. Nicholson-Ross-Weir and New Non-Iterative conversions methods are selected since both methods supports waveguide based measurements, and are also applicable to planar surfaces with good accuracy of computing relative permittivity and dielectric loss tangent. Convergence method results are discussed in upcoming section.

4.1. Nicholson-Ross-Weir(NRW) conversion method NRW conversion method is the most

glitches in the complete frequency band indicate proper manufacturing of both composite samples and test adapters. Now we can proceed for the calculation of relative permittivity (εr) and dielectric loss tangent(tanδ)

4. Calculation of permitivitty& dielectric loss tangent of GFRP composite samples Relative permittivity and dielectric loss tangent of the samples are calculated using two convergence methods.

commonly used conversion method to calculate the relative permittivity (εr) and permeability (μr) of any material using scattering parameters. NRW conversion method is fast and non-iterative and is applicable to waveguide based measurements performed. In order to calculate the relative permittivity, Transmission coefficient (T) is calculated using equation (1).

$$T = \frac{S_{11} + S_{21} - \Gamma}{1 - (S_{11} + S_{21})\Gamma}$$

Where, 'Γ' is the reflection coefficient and is calculated using (Γ = X+ *X*2 - 1). MATLAB script of NRW
conversion is written in order to compute the Transmission Coefficient. Relative

IJFANS INTERNATIONAL JOURNAL OF FOOD AND NUTRITIONAL SCIENCES
ISSN PRINT 2319 1775 Online 2320 7876
 Journal Volume 11, Iss 09, 2022

permittivity is then calculated using equation (2).

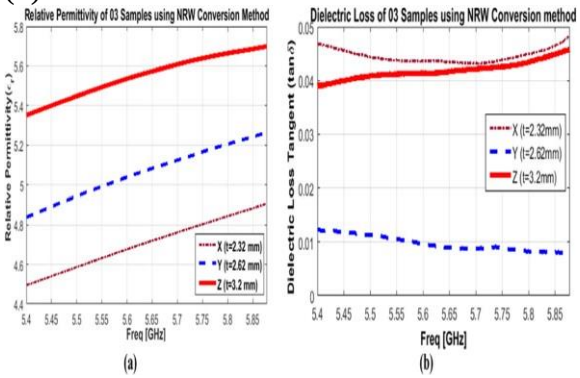

$$\varepsilon_r = \frac{\lambda_o^2}{\mu_r}\left(\frac{1}{\lambda_c^2} - \left[\frac{1}{2\pi t}\ln\left(\frac{1}{T}\right)\right]\right)$$

Where, 'λ0' is the free space wavelength and 'λc' is the cut off frequency wavelength. WR-187 has an operating frequency band from 3.95 to 5.85 GHz. Cutoff frequency in this case is considered as 3.95 GHz. 't' is the thickness of the sample and in this case, all 03 samples tested are of different thicknesses as reported in table 1. Using equations(1) and (2), relative permittivity (εr) is calculated and reported in figure 5 for all 03 samples.

By analyzing relative permittivity in figure 5(a), Sample-Z with a thickness of 3.2 mm has the highest relative permittivity throughout the frequency range as compared to Sample-X and Sample-Y. Sample-X with the least thickness of 2.32 mm as compared to Sample-Y and Sample-Z exhibits the lowest relative permittivity. For metasurface antenna applications, in which electromagnetic waves needs to radiate, require a surface with the low permittivity. Results illustrates that Sample-X with 2.32 mm thickness is a suitable candidate compared to other 02 samples to be used a metasurface. Thickness of the sample could also have been further reduced in order to further achieve a lower relative permittivity but further reduction of thickness may result in less stiffness and may result in deformation of the sample. NRW conversion method results are validated using New Non Iterative conversion method discussed in the subsequent section.

4.2. New non iterative conversion method

New Non-Iterative method is similar to NRW method but with a different formulation. This method is also suitable for permittivity calculation. This method is fast and non-iterative and no initial guess is needed for relative permittivity calculation. This conversion method also supports waveguide based measurements.

Transmission coefficient 'T' is calculated using equation (1) and relative permittivity is calculated by equation (3).

$$\varepsilon_r = \left[1 - \frac{\lambda_o^2}{\lambda_c^2}\right]\varepsilon_{eff} + \frac{\lambda_o^2}{\lambda_c^2}\frac{1}{\mu_{eff}}$$

Where, 'εeff' and 'μeff' is the effective permittivity and permeability respectively and is calculated using equations(4) and (5),

Where, 'εeff' and 'μeff' is the effective permittivity and permeability respectively and is calculated using equations(4) and (5),

Where 'Λ' is calculated using equation (6),

$$\frac{1}{\Lambda^2} = -\left[\frac{1}{2\pi t}\ln\left(\frac{1}{T}\right)\right]^2$$

Calculated values of εeff, μeffandΛare substituted in equation (3) and relative permittivity is calculated over the complete frequency range. Figure 6 shows the relative permittivity and dielectric loss tangent plots of all 03 samples using New Non-Iterative Conversion method;

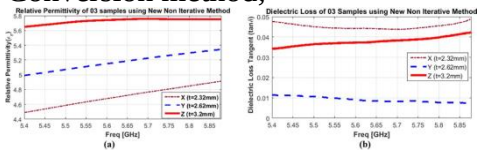

Table 2. Relative Permittivity and Dielectric Loss Tangent of GFRP composite samples.

Sample	Layers (No.)	Thickness (mm)	Frequency (GHz)	Relative Permittivity (ε_r)	Dielectric Loss Tangent (tanδ)
X	5	2.32	5.4 to 5.9	4.5 ~ 4.9	0.042 ~ 0.049
Y	15	2.62		4.83 ~ 5.32	0.008 ~ 0.012
Z	25	3.2		5.35 ~ 5.75	0.035 ~ 0.045

By analyzing the relative permittivity in figure 6(a), similar relative permittivity curves are observed for all 03 samples by using New Non Iterative method in comparison to NRW method. Similarity in computed relative permittivity using both conversion methods indicates that the conversion methods are applicable for this type of waveguide based measurement performed. Plots of relative permittivity for all 03 samples shown in figures 5(a) and 6(a) also indicate relative permittivity value is increasing with the increase of frequency and

ISSN PRINT 2319 1775 Online 2320 7876
 Journal Volume 11, Iss 09, 2022

number of layers in the sample. In order to use a low relative permittivity composite sample for metasurface antenna application [28], based on the findings in this paper, number of fibermat or fiber peel ply layers should be as minimum as possible. Dielectric loss tangent of all the GFRP based composite samples shown in figures 5(b) and 6(b) varies from 0.01 to 0.05 which is in a good agreement with hybrid composites developed using natural fiber[29]. table 2 shows the summarized data of all 03 GFRP composite samples; By analyzing table 2, Sample-X exhibits lowest permittivity over the complete frequency range as compared to Sample-Y and Sample-Z. Sample-X having a thickness of 2.32 mm with 05 layers and with a computed relative permittivity (εr) of 4.72 and dielectric loss tangent (tanδ) value of 0.045 at a center frequency of 5.65 GHz is suitable to be used for the design of metasurface antenna.

5. CONCLUSION

In this paper, fabricated GFRP based composite polymers are evaluated for the feasibility as a metasurface antenna. GFRP using chopped E-Glass fiber mat and E-glass fiber peel ply are fabricated using VARTM technique and then successfully characterized using specially designed test jigs. Relative permittivity and dielectric loss tangent of each sample is successfully calculated with the help of NRW and Non-Iterative conversion method with great similarity of results between both methods. Results of all samples indicates that the sample with less number of layers provides lowest relative permittivity. Finally, Sample-X (Chopped E-Glass Fiber mat)with 05 layers having relative permittivity of 4.72 is selected for use in metasurface antenna applications. Future work involves printing of unit cells on the selected composite sample and then use as a metasurface on a patch antenna resonating in the same frequency band from 5.4 to 5.9 GHz. Goal will be the electromagnetic performance enhancement (bandwidth, gain, frequency reconfiguration) of patch antenna using GFRP based composite as a metasurface.

REFERENCES

[1] Bannister M 2001 Challenges for composites into the next millennium - a reinforcement perspective Composites Part A: Applied Science and Manufacturing 32 901–10

[2] Satyanarayana K G, Pai B C, Sukumaran K and Pillai S G K 1990 Fabrication and Properties of Lignocellulosic Fiber—Incorporated Polyester Composites Handbook of Ceramics and Composites (Synthesis and Properties) 1 (New York: Marcel Decker Inc.) 339–84

[3] Clyne T W and Hull D 2019 An Introduction to Composite Materials 3rd edn(Cambridge, UK: Cambridge University Press)

[4] Zagho M M, Hussein E A and Elzatahry A A 2018 Recent overviews in functional polymer composites for biomedical applications Polymers 10 739

[5] Monteiro S N, de Assis F S, Ferreira C L, Simonassi N T, Weber R P, Oliveira M S, Colorado H A and Pereira A C 2018 Fique fabric: a promising reinforcement for polymer composites Polymers 10 246

[6] Movahedi N and Linul E 2017 Quasi-static Compressive Behavior of the ex situ Aluminum-alloy Foam-filled Tubes under Elevated Temperature Conditions 206 182–4

[7] Holloway C L, Kuester E F, Gordon J A, O'Hara J, Booth J and Smith D R 2012 An Overview of the Theory and Applications of Metasurfaces. The Two Dimensional Equivalents of Metamaterials 54 10–35

[8] Oscar Q-T et al 2019 J. Opt. 21 073002

[9] Zhu H L, Cheung S W, Guo Y J, Ding C and Yuk T I 2016 Aperture efficiency improvement using metasurface10th European Conference on Antennas and Propagation (EuCAP) (Davos) pp 1–3

[10] Zhu H L, Liu X H and Chuencg S W 2014 Frequency re-configurable antenna using metasurfaceIEEE Transactions on Antenna & Propagation 62 80–5

[11] Sivakumar E, Ramachandran B and Priyadharshini G 2015 Metasurface antenna with switchable polarization International

ISSN PRINT 2319 1775 Online 2320 7876
 Journal Volume 11, Iss 09, 2022

Conference on Communications and Signal Processing (ICCSP) (Melmaruvathur) pp 1875–80
[12] Pan Y M, Hu P F, Zhang X Y and Zheng Y 2016 A low profile high gain and wideband filtering antenna with metasurfacesIEEE Transactions on Antenna & Propagation 64 2010–6
[13] Gatea Q M et al 2020 J. Phys. Conf. Ser. 1664 012022
[14] Bakar H A et al 2018 J. Phys. Conf. Ser. 1049 012083
[15] Zhu H, Chung K L and Sun L 2012 CP metasurfaced antennas excited by LP sources Antennas and Propagation Society International Symposium, IEEE Symposium
[16] Morsli M, Bonnet A, Samir F and Lefrent S J 1996 Appl. Poly. Sci. 61 231
[17] , A. K., Laxmaiah, G., & Babu, P. R. Process Parameters Optimization And Characterization Of RTM Manufacturing Process For High Performance Composites. Polym. Compos. Sci. 1 138–51
[18] Perna A S, Viscusi A, Astarita A, Boccarusso L, Carrino L, Durante M and Sansone R 2019 Manufacturing of a metal matrix composite coating on a polymer matrix composite through cold gas dynamic spray technique J. Mater. Eng. Perform. 28 3211–9
[19] Carruthers J 2018 Vacuum Bagging Process Overview, Coventive Composites https: /coventivecomposites.com/explainers/what-is vacuum-bagging/
[20] Ahmad N, Bilal I and Khattak S 2018 Polyester usage in manufacturing of electrical and mechanical products and assemblies Polyest. Prod. Charact. Innov. Appl. ed N O Camlibel(Rijeka: IntechOpen) ch 4 (https://doi.org/10.5772/intechopen.74368)
[21] Kumar, A. K. A managerial approach towards reliable maintenance of high productive machine.
[22] Kumar, A. K., Laxmaiah, G., & Babu, P. R. Process Parameters Optimization And Characterization Of RTM Manufacturing Process For High Performance Composites.
[23] Yaw K C 2012 Measurement of Dielectric Material Properties(Rohde & Schwarz) Application Note
[24] Nicolson A M and Ross G 1970 Measurement of the intrinsic properties of materials by time domain techniquesIEEE Trans. Instrum. Meas. 19 377–82
[25] Weir W B 1974 Automatic measurements of complex dielectric constant and permeability at microwave frequencies Proc. IEEE 62 33–6
[26] Kim S, Kuester E F, Holloway C L, Scher A D and Baker-Jarvis J 2011 Boundary effects on the determination of metamaterial parameters from normal incidence reflection and transmission measurementsIEEE Transactions on Antennas and Propagation, AP-59 6 2226–40
[27] Rohde & Schwarz ZVA Vector Network Analyzer, Test & Measurement, Operating Manual, Open Source (1145.1084.12-24)
[28] Faenzi M, Minatti G, González-Ovejero D, Caminita F, Martini E, Della Giovampaola C and Maci S 2019 Metasurface antennas: new models, applications and realizations Sci. Rep. 10178 1AB